

Accelerating micromodeling in oil田 injection in high-adhesion oil fields based on high fame of coreele

Jingjie Cao^{1,4} Yanfei Wang² Benfeng Wang³

¹Shijiazhuang University of Economics, Shijiazhuang, Hebei 050031, China.

²Key Laboratory of Petroleum Resources Research, Institute of Geology and Geophysics, Chinese Academy of Sciences, PO Box 9825, Beijing 100029, China.

³State Key Laboratory of Petroleum Resources and Prospecting, China University of Petroleum, Beijing 102249, China.

⁴Corresponding author. Email: cao18601861@163.com

Abstract. Seismic interpretation, a key technique for identifying oil reservoirs, is a complex process involving multiple steps and requires significant expertise. The workflow typically includes data acquisition, processing, interpretation, and validation. In this study, we propose a new workflow for seismic interpretation of high-adhesion oil fields. The workflow consists of five main stages: data acquisition, processing, interpretation, validation, and application. The proposed workflow is designed to be more efficient and accurate than traditional methods, particularly for high-adhesion oil fields where conventional methods often fail. The proposed workflow involves the use of advanced seismic processing techniques, such as full-waveform inversion and migration, to improve the quality of seismic data. The interpretation stage involves the use of machine learning algorithms to identify oil reservoirs based on seismic features. The validation stage involves the use of geological and petrophysical data to verify the interpreted results. The application stage involves the use of the interpreted results to guide oil田 injection operations. The proposed workflow has been successfully applied to several high-adhesion oil fields, resulting in improved oil recovery rates and reduced costs.

Keywords: seismic interpretation, oil田 injection, seismic interpretation, L1 regularization, aefield

Received 11 February 2014, accepted 24 June 2014, published online 6 August 2014

Introduction

Seismic interpretation is a key technique for identifying oil reservoirs. It involves the analysis of seismic data to determine the presence and characteristics of oil reservoirs. The workflow typically involves data acquisition, processing, interpretation, and validation. In this study, we propose a new workflow for seismic interpretation of high-adhesion oil fields. The proposed workflow is designed to be more efficient and accurate than traditional methods, particularly for high-adhesion oil fields where conventional methods often fail.

The proposed workflow involves the use of advanced seismic processing techniques, such as full-waveform inversion and migration, to improve the quality of seismic data. The interpretation stage involves the use of machine learning algorithms to identify oil reservoirs based on seismic features. The validation stage involves the use of geological and petrophysical data to verify the interpreted results. The application stage involves the use of the interpreted results to guide oil田 injection operations. The proposed workflow has been successfully applied to several high-adhesion oil fields, resulting in improved oil recovery rates and reduced costs.

Seismic interpretation is a key technique for identifying oil reservoirs. It involves the analysis of seismic data to determine the presence and characteristics of oil reservoirs. The workflow typically involves data acquisition, processing, interpretation, and validation. In this study, we propose a new workflow for seismic interpretation of high-adhesion oil fields. The proposed workflow is designed to be more efficient and accurate than traditional methods, particularly for high-adhesion oil fields where conventional methods often fail.

The proposed workflow involves the use of advanced seismic processing techniques, such as full-waveform inversion and migration, to improve the quality of seismic data. The interpretation stage involves the use of machine learning algorithms to identify oil reservoirs based on seismic features. The validation stage involves the use of geological and petrophysical data to verify the interpreted results. The application stage involves the use of the interpreted results to guide oil田 injection operations. The proposed workflow has been successfully applied to several high-adhesion oil fields, resulting in improved oil recovery rates and reduced costs.

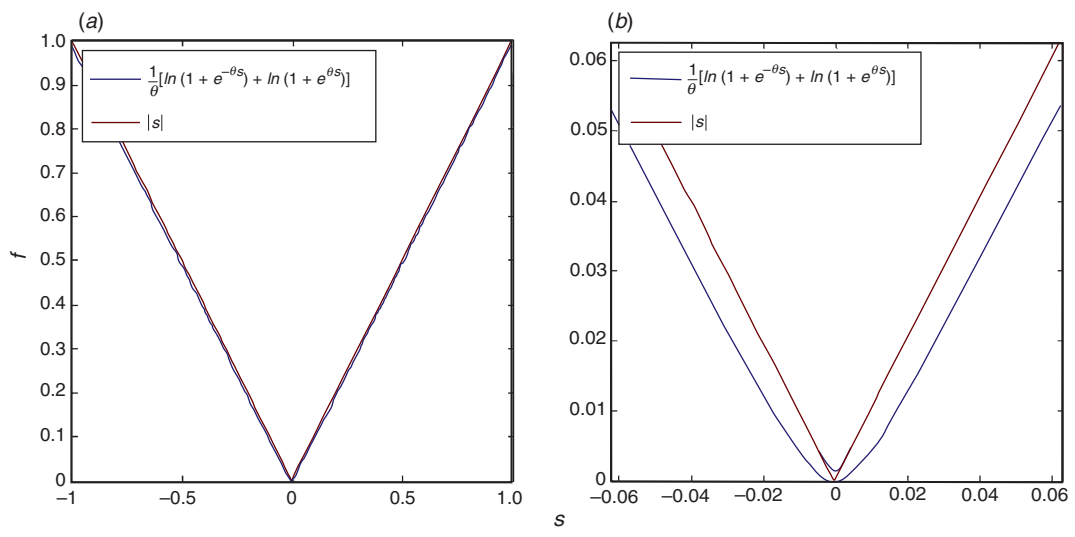
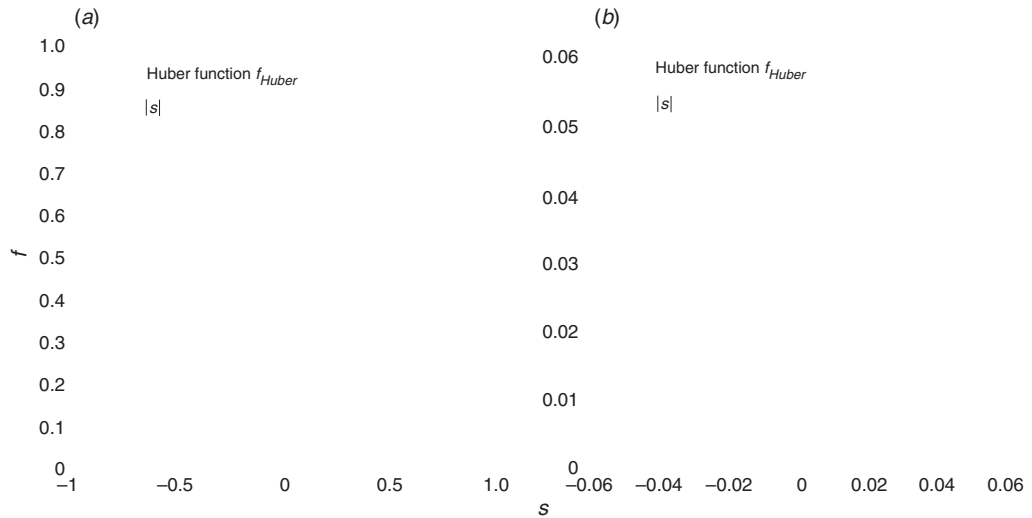


Figure 2. The Huber function f_{Huber} is magnified near the origin. The Huber function is smooth at $s=0$, while the absolute value function has a sharp corner.



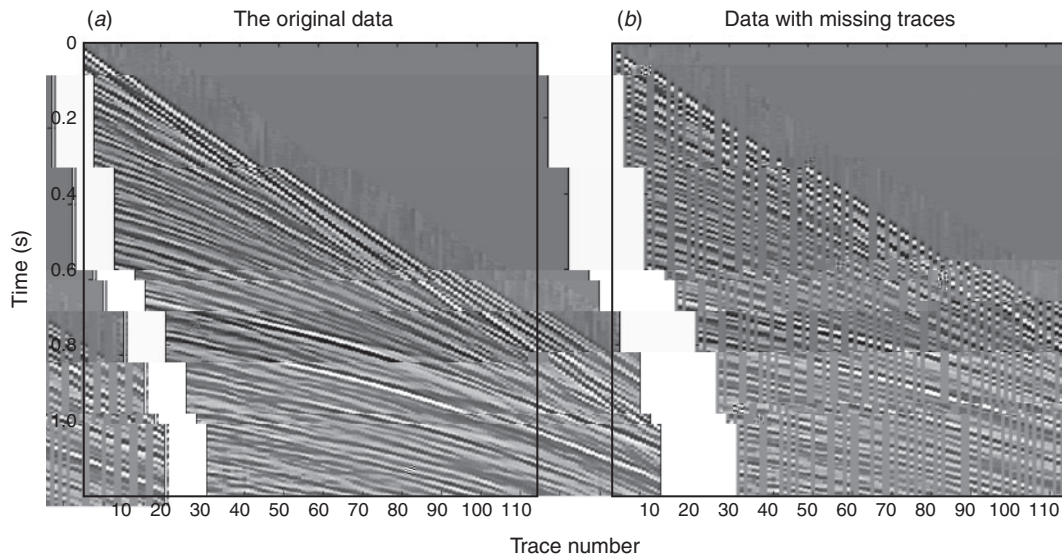


Fig. 4. (a) Original data. (b) Data with missing traces.

Table 1. Comparison of L₁, FISTA and SPGL1 methods.

	S	h L ₁	FISTA	SPGL1
CPU time (s)	56	73	156	
SNR (db)	10.4975	9.8556	9.9523	
Relative error	0.2986	0.3215	0.3180	

ca be a pied a d he eg la i a i a a e e i e e i ed ba ed he g adie jec i h d i h h L₁ n a i a i . I hi a e , e h L₁ f ci a e a q ed fi , he he H be f ci i ch e a n i a e he L₁ . A c qe -ba ed fa g adie jec i e h d i ed 1 e he e q i c ai ed h L₁ i a i . The q f he ed e h di he e f he igh f a e n e f he c qe a f ed ce he c a i a q c . N e i c a q e a le h e i c a d e q ei ic da a de n a e he qidi f he n ed h d.

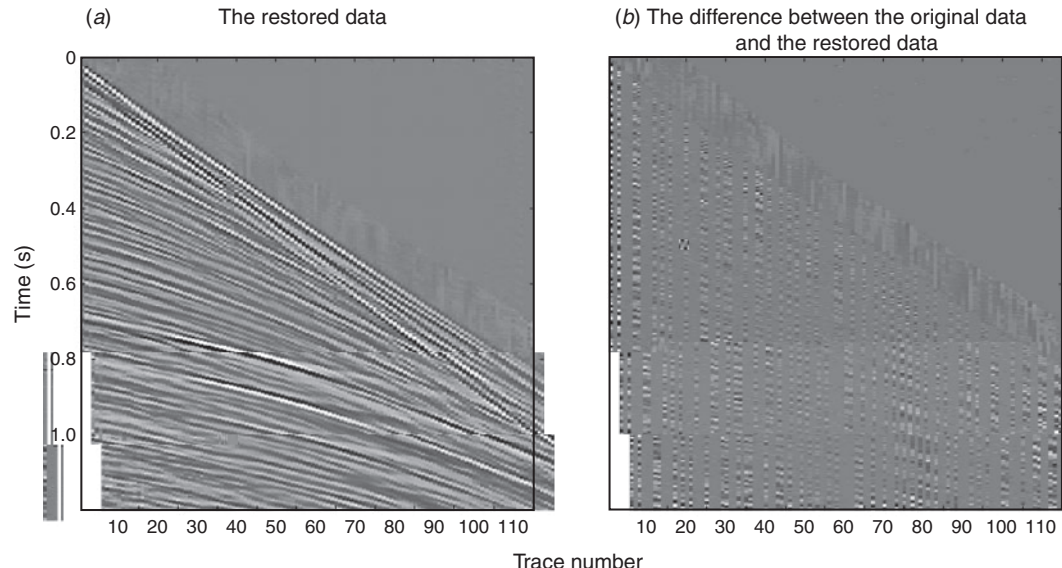


Fig. 5. (a) Restored data. (b) Difference between the original data and the restored data.

Seismic imaging model of seismic sparse interpolation

Mathematical model of seismic sparse interpolation
 Seismic imaging model of seismic sparse interpolation

$$\Phi = \dots, \quad (1)$$

he e Φ de e he a l i g ce i g, i he c jee ei ic da a, a d, i he a led da a. Th e a e i fi i q a l i he n ca l, b e ca i i e e f f a i fi d he l i ih h n ca ea i g. S a i f he ei n ic da a i a f ed d ai n c l ed beca e ei n ic e e n ca be a q e e ed b e a f . F ei n ic ce i g, e fa i jia a f a e he F ie a f (Li, 2004; Z a je a d Sacchi, 2007), he jie Rad n a f (Tade a q., 2002), he a ab jic Rad n a f (Dache, 1990) a d he c qe a f (He a n a d He e fe, 2008). Rec e l, Ga ia rbea ha e bee n ad ed f n el ic da a dec n i i n (Li e q.,

2013; W a g e q., 2013). If $\Phi = \Psi^* \Phi \Psi^* = \Phi \Psi^* \Phi^* = \Phi \Psi^*$, (2)

he e $\Psi^* \Phi$ i he He iia a e f Ψ ad = $\Phi \Psi^*$. Ma
e h d ha e bee de q ed fi d a e l i e a i f
2, cha g ee d q g i h (Mall a a d Zha g, 1993), c e
i i a i (Bec a d Teb ll e, 2009; a de Be g a d
Fieq a de, 2009; Che e q., 1998) a d n -c h e
i i a i (M hi a i e q., 2009). C e n i a i
e h d i h he e i a l i ig j ifica i a e i a b e
f ja ge- ca e c a i (Ca e q., 2012; Che e q.,
1998). The c n ed c n e i i a i h i he
ba i . i b e :

$$\|_1 \| \|_1 \dots = . , \quad (3)$$

hich ca be a f ed i li ea i i a i a d l ed b
he i e f i h e h d (Che h e q., 1998; Ca h de a h d Ta ,

2005). Beca e he bjec i e f ci n fe ai 3 i
diffe e iaq e a igi, i ca n be l ed b h e c n j n ga e
g adie h e h d a d Ne n e e h d di ec l . He ce,
e ea che ha e n ed n l e he h c n ai ed f n f
e a i n 3:

$$\|_1 \| \|_1^2 + \lambda \|_1 , \quad (4)$$

i g f e a je he IST a d FISTA e h d , b he
eg la i a i a a e e \lambda \|_1 d be adj ed ca ef ll .
A he a eg e c e he -diffe e iabji f
e a i 3 i elaci g he L_1 n b h i h
a i a i , hich ca be ca led he h L_1 e h d.
Th , e a i n 3 ca be cha ged i h

$$\|_1 () \dots = . , \quad (5)$$

he e () i a h a i a i f he L_1 . I he
f ll i g, e h L_1 n f h c i n a e d c ed a d
a q ed.

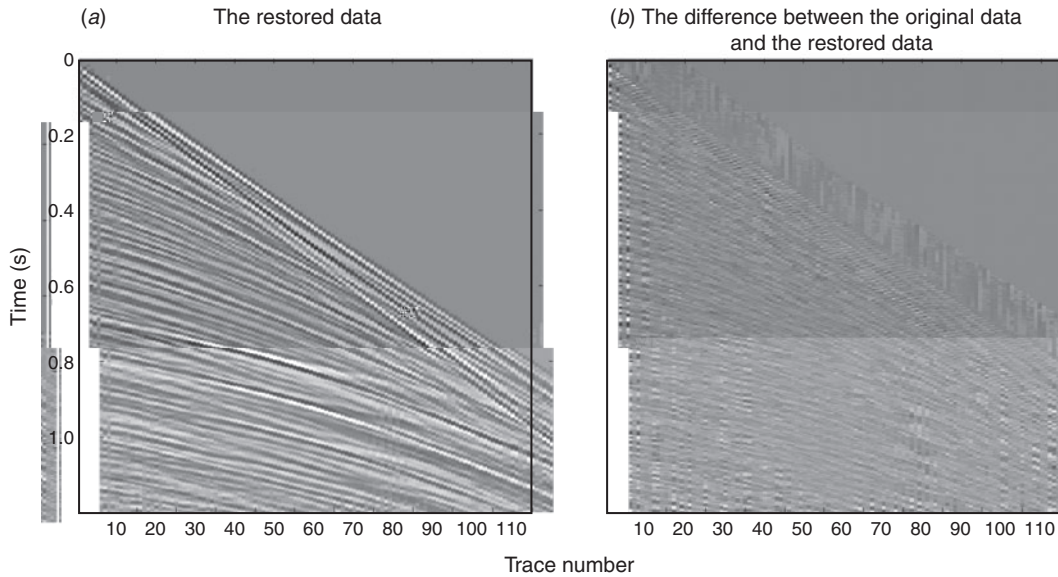


Fig. 6. (a) The restored data by FISTA and (b) the difference between the original data and the restored data.

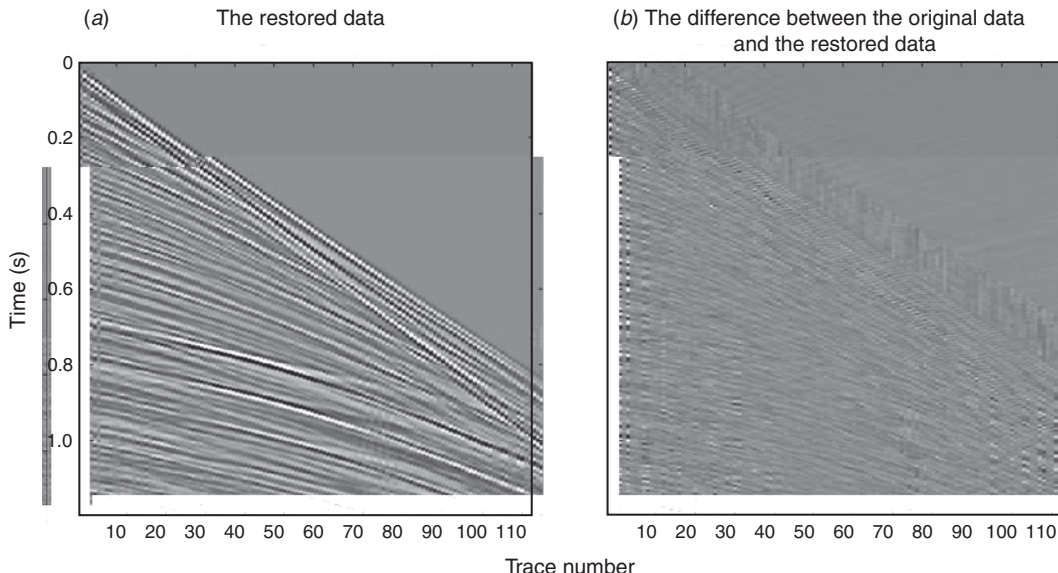


Fig. 7. (a) The restored data by SPGL1 and (b) the difference between the original data and the restored data.

Comparison of smooth L_1 norm functions

S h L₁ f c i a e h a i a i f he L₁
 hich a e e ^f a b ^f e a d ca be i e a () ^f $\sum_{n=1}^{\infty}$ (),
 ej eed a q e he 1D ^f ca e (), he e i a cq a . The
 fi f c f ^f e df c i

$$_{\varepsilon}(\) = \sqrt{^2 + \varepsilon} \quad (6)$$

A recent study by Wang et al. (2011) indicated that the effect of water availability on plant growth and yield is significant. The results showed that as water availability decreased, plant growth and yield decreased significantly. This study also found that the effect of water availability on plant growth and yield was more pronounced at higher temperatures. The results suggest that water availability is a key factor in determining plant growth and yield, and that it is important to manage water availability to optimize plant growth and yield.

The ^h ec _h d f _h c i _h i

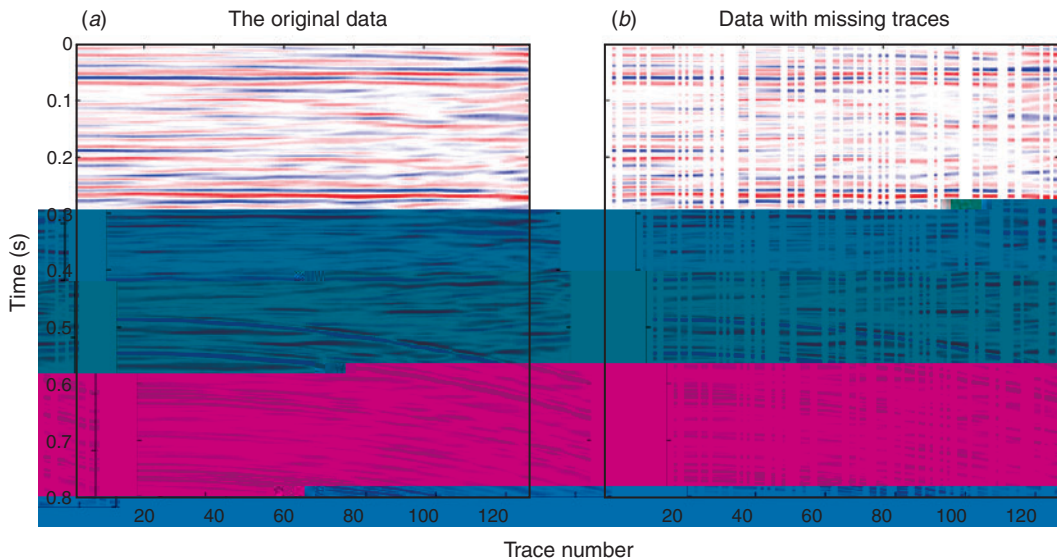
$$\theta(\) = \frac{1}{\theta} [l_n(1 + e^{-\theta}) + l_n(1 + e^{\theta})], \quad (7)$$

which a i a e e eq he θ i la gee gh. Thi
f n c i n i c n e a d diffe n iq (Che n a d Ma n ga a ia n

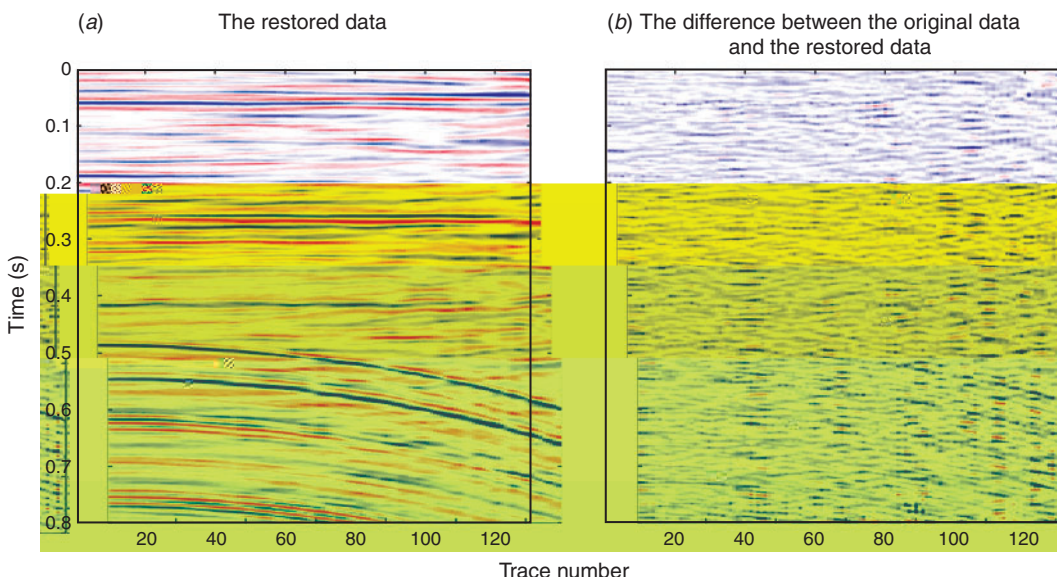
1996). A I f i i g e i Fig e 2 i h $\theta = 10000$.
 Fig e 2 i a ag ified h f Fig e 2 . A i h
 Fig e 1 , i i q h - e a h g i q j .
 A h h e f a f h c i h i h H b h f h c i h :

$$H_{\text{be}}(\text{ }) = \begin{cases} ^2/2, & \text{if } | | \leq \\ | | - /2, & \text{q e } | | > \end{cases} . \quad (8)$$

I e a i 8, i c a l l e d a e - a a e e . The H be f ^l_c i i h he e he e a d a a c h e e e q ^{ll} h e e (B b e a ^d N e e h, 2007). I i l edi Fig e 3 ^h i h ^h = 0.0001; a a g ^l ified ie h ha i e a ^q e e ac l a he ig i q i . The H be f c i i a h b id f he L₁ a d h e L₂ ^h; i beha e l i e h e L₂ ^h f a q l a d l i e h e L₁ ^h f l a g e . The h a ^h i i f L₂ n L₁ ^h beha i i c l l e d b . H b e f c i a e n e ^h ge h i c a i e ^h e b e ; Sacchi ^h ed he Ca ch f c i a d H b e f c i f dec l i ge a e effec i f e ie (Sacchi, 1997). He e, e a ^h i a a e a e e ge a e l i f ei ic i e lai .



Fz. 8. () O igi _b q ac da a. () Sa 1ed ac da a.



F₂.9. () I₁ e la i₁ f ac da a b h L₁ e h d. () Diffe₁ e₁ ce be ee₁ () a₁ d igi₁ a₁ ac da a.

Ba ed he ab edic i , ec q i ca be
ade: (1) A^T e - a a e e e i n each f c i c l he
a i ai , ad he a eq diffe hq; (2) $e(A^T)$ d o()
a e e ac h e h igi q i , h i g e H be()e a
e h a he igi q i a dca h a hach he L₁ be e
f gi e e h a a h e h . The ef e, H be()i ch e a he
L₁ h a i ai n . Re i i g e a i n 5 i g he H be()
c h ai h iq d

$$i_n(\cdot) := \sum_{l=1}^n h_b(\cdot) \dots = \dots \quad (9)$$

E ai 9 i a a a f ed i a c ai
b e , i hich he eg la h a i fac h h d be ch e
ca ef ll . de a id he eg la h a i fac , he g adie h
jec i e h d, hich i a e efficie h a eg , i ed h
1 e he c h ai ed i i ai h .

Gradient projection method for smooth L_1 norm optimisation

Si ce e ai 2 i de de e i ed, = = i ac e
e h e a i 9 c a be l ed b a c e e jec i
e h d. A g adie h jec i n aq g i h f e a i n 9 h
de ig a ed a f ll :

Gi e he a i i e a i , he a a e e = 0.0001,
= 0, a d he i i ia l i o. If he i g c i e i i
a i fied, g S e 4; he i e, g i e a i i a i e a i
+1 = $-\mu \nabla (\cdot)$, he e mu i he e le g h (hich ca h
be l ed b bac - aci g e h d).
U da e he i e a i n i : +1 = +1 - (+1)
(+1) i.e. jec i n = n = , ie = +1,
= +1, a d e S e t 2.
Gi e he fi q l i n : = .

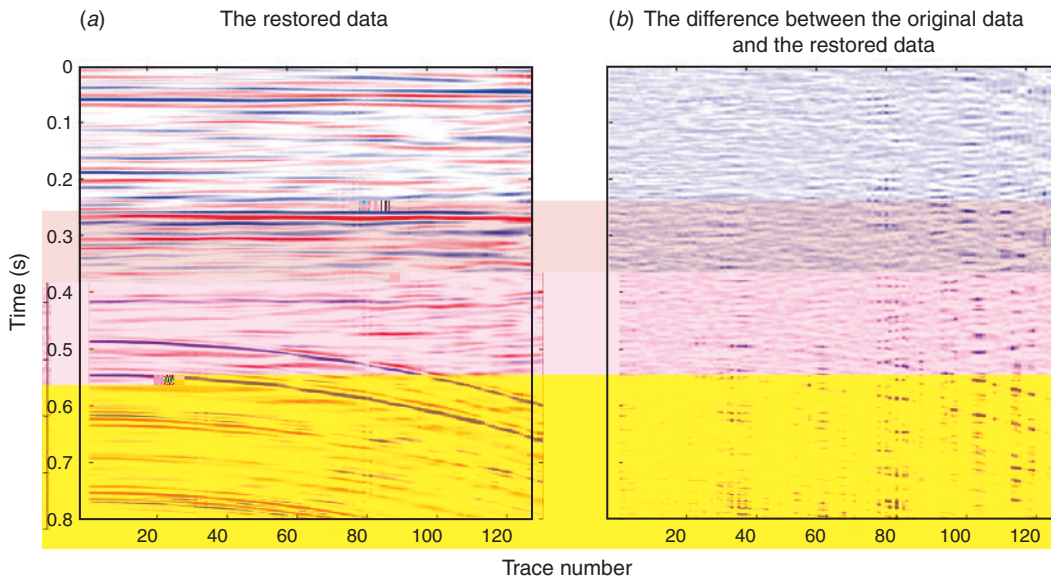


Fig. 10. (a) The restored data using FISTA and (b) The difference between the original data and the restored data.

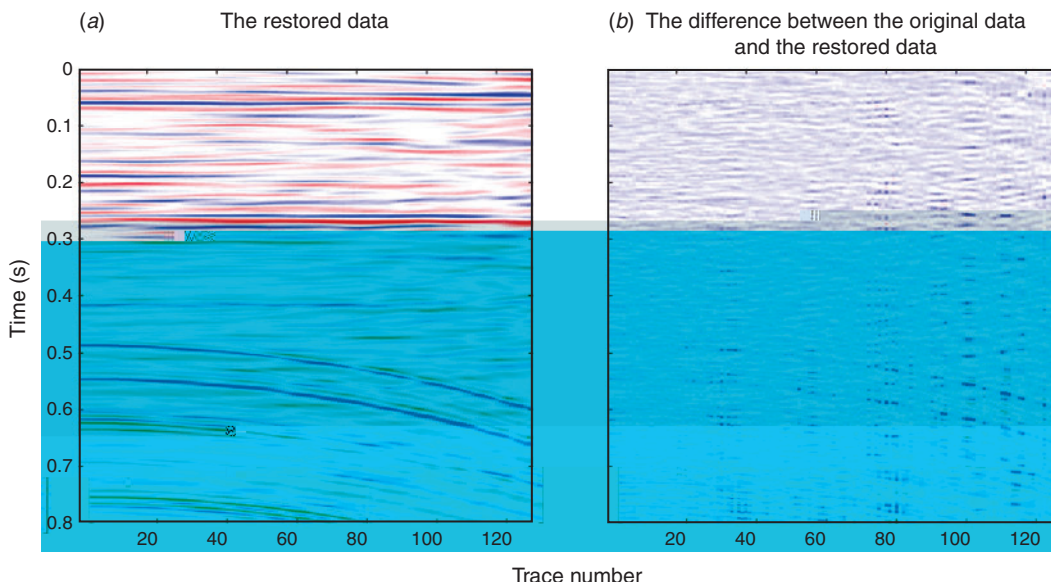


Fig. 11. (a) The restored data using SPGL1 and (b) The difference between the original data and the restored data.

Table 2. Comparison of L₁, FISTA and SPGL1 methods

	S	hL ₁	FISTA	SPGL1
CPU time()		56	80	163
SNR (db)		22.1805	22.7094	22.9518
Relative error		0.0778	0.0732	0.0712

We choose the regularization parameter $\lambda = \sqrt{\frac{1}{\text{SNR}}}$ (Wang et al., 2011). The initial \mathbf{x}_0 is set to zero. The iteration number is 300.

The algorithm starts with the initial guess \mathbf{x}_0 . The update rule is given by (3)–(5). The iteration process continues until the relative error is less than a tolerance value. The final solution is obtained after 300 iterations. The CPU time is approximately 56 seconds. The SNR is approximately 22.1805 dB. The relative error is approximately 0.0778. The results show that the proposed method is efficient and accurate.

The curvelet transform

Because of the sparsity of seismic data, we can use the curvelet transform to represent the data. The curvelet transform is a multi-scale and multi-directional representation of seismic data. It is based on the wavelet transform and the Radon transform. The curvelet transform has been shown to be effective for seismic data processing (Candès et al., 2006; Candès and Donoho, 2004). The curvelet transform is particularly useful for seismic data denoising and deconvolution. The proposed method uses the curvelet transform to represent the seismic data and then applies the L₁-norm minimization to recover the sparse coefficients. The results show that the proposed method is efficient and accurate.

Numerical example

The proposed method is applied to a synthetic seismic dataset. The dataset consists of a single trace with 128 samples. The sampling rate is 20 Hz. The trace is recorded over a distance of 1000 m. The source is located at the surface. The receiver is located at a depth of 500 m. The source wavelet is a Ricker wavelet with a center frequency of 10 Hz. The receiver wavelet is a Ricker wavelet with a center frequency of 15 Hz. The seismic data is simulated using a finite-difference method. The seismic data is noisy. The noise level is approximately 10 dB. The seismic data is processed using the proposed method. The results show that the proposed method is able to recover the sparse coefficients of the seismic data.

Shot data experiment

A shot data is recorded over a distance of 1000 m. The source is located at the surface. The receiver is located at a depth of 500 m. The source wavelet is a Ricker wavelet with a center frequency of 10 Hz. The receiver wavelet is a Ricker wavelet with a center frequency of 15 Hz. The seismic data is noisy. The noise level is approximately 10 dB. The seismic data is processed using the proposed method. The results show that the proposed method is able to recover the sparse coefficients of the seismic data.

69 acre. The image quality is Fig. 4, and the results are shown in Fig. 4. We compare the results obtained by L₁, FISTA (Bach and Teboulle, 2009) and SPGL1 (Chen et al., 2009). The results are shown in Table 1. The SNR is defined as:

$$= 10 \log_{10} \frac{\|\mathbf{y}\|_2^2}{\|\mathbf{y} - \mathbf{x}\|_2^2}$$

he image quality is defined as the SNR defined as:

$$\frac{\|\mathbf{y} - \mathbf{x}\|_2}{\|\mathbf{y}\|_2}$$

The image quality is defined as the SNR defined as:

Post-stack seismic data experiment

We compare the results obtained by L₁, FISTA and SPGL1. The results are shown in Table 1. The SNR is defined as:

Conclusion

In this paper, we propose a new method for seismic data processing. The proposed method is based on the curvelet transform and the L₁-norm minimization. The proposed method is able to recover the sparse coefficients of the seismic data. The results show that the proposed method is efficient and accurate.

ed e h d i he fa e a g he h ee e h d . The ef e, i ca be ed i e he efficie c f ei ic ce i g, e ncial f high di e i a h ei ic da a i e l a i . The ed e h d i ba ed he c qe a f bai he i e la ed ei ic da a hich i a ed da c a f a d i ec i g, he ef e i abef l a ge ga . F e each e efficie a e a f (T ad, 2009), e ncial efficie high di e i a h ei , i e i ed. The L c ai a d i h a i a i a d i h be he be a ec ai . The ef e, he a ec i a i , i e he L (0 < f) h d be i e ig a ed f he .

Ackno ledgmen

We ha P fe M. D. Sacchi a d a a efe ee f hq f l gge a d hei edi i g f he a e . We a ldi e ha he a h fC qaba dS a c f a i g hei c de a ajab e . Thi i ed b Nai a Na a Scie c F dai f Chi a de g a be 41204075, 41325016 a d 11271349, a d Nai a Scie c F dai f Hebei P i ce de g a be D2014403007.

Refence

- Ab a,R.,a dKabi ,N.,2006,3Di e lai fi egla da a ihaPOCS ag i h : ,71, E91–E97. d i:10.1190/1.2356088
- Bec , A., a d Teb ll e, M., 2009, A fa i a i e h i -he h l d i g ag i h f i ea i e e b e : I , 2, 183–202. d i:10.1137/080716542
- B be, K., a d Ne e h, T., 2007, Fa i i e ea che f he b . 1. i f i ea h e i heh bida dH b e : , 72, A13–A17. d i:10.1190/1.2431639
- Ca de , E., 2006, C e i e a l i g: , I , E ea Mahe aicq S cie P bi hi g H e, 33–52.
- Ca de , E., a d D h , D., 2004, Ne igh fa e f c qe a d i q e e n a i f bjec i h iece i e i g la i i e : , 57, 219–266. d i:10.1002/c a.10116
- Ca de , E., a d Ta , T., 2005, Dec di g b i ea g a i g: I , 51, 4203–4215. d i:10.1109/ TIT.2005.858979
- Ca , J., Wa g, Y., a d Ya g, C., 2012, Sei ic da a e a i ba ed c e i e e n g i g eg la i a i a d e e a e i i a i : , 55, 239–251. d i:10.1002/ cje2.1718
- Che , C., a d Ma ga a ia , O., 1996, A qa f hig f c i f n n i ea a d i ed c i e e a i b e : , 5, 97–138. d i:10.1007/BF00249052
- Che , S., D h , D., a d Sa n de , M., 1998, A ic dec i i b ba i i : I , 20, 33–61. d i:10.1137/S1064827596304010
- Da che, G., 1990, S a i q i e lai i g a fa a ab lic a f : 60 h A a q I e a i a Mee i g, SEG, E a ded Ab ac , 1647–1650.
- D ij da , A., Sch e i e, M., a d Hi d i , C., 1999, Rec c i f ba d i i ed ig q , i eg la i a i ed q g e a i q di ec i : , 64, 524–538. d i:10.1190/1.1444559
- He a n , F., a d He e fe , G., 2008, N a a e ic ei ic da a ec e , i h c qe fa e : , 173, 233–248. d i:10.1111/j.1365-246X.2007.03698.
- Ke i e , N., a d Sacchi, M., 2012 , A e hig a a e dec i i (HOSVD) f e ac ei ic da a i e ed ci a d i e la i : , 77, V113–V122. d i:10.1190/ge 2011-0399.1
- Ke i e , N., a d Sacchi, M., 2012 , Rec c i f ei ic da a i a e c i e i : , 29, 29–32.
- Ke i e , N., a d Sacchi, M., 2013, Te c i e i ba ed h qea i i i a i f 5D ei ic da a ec c i : , 78, V273–V284. d i:10.1190/ge 2013-0022.1
- Li , B., 2004, M i di e i a q ec c i f ei ic da a: Ph.D. he i , U i e i f A i be a.
- Li , P., Wa g, Y. F., Ya g, M. M., a d Ya g, C. C., 2013, Sei ic da a dec i i i g a e Ga ia bea : , 56, 3887–3895.
- Ma jia , S., a d Zha h g, Z., 1993, Ma ch i g i i h i e f e e dic i a ie : I , 41, 3397–3415. d i:10.1109/78.258082
- M hi a i, H., Babaie-Zadeh, M., a d J e , C., 2009, A fa a ach f e-c i e a e dec i i ba ed hed o : , 57, 289–301. d i:10.1109/TSP.2008.2007606
- Naghadeh, M., a d Sacchi, M., 2010, Be d a i a hie a chiq c a e c qe i e lai f eg lai a d i h eg lai a ied ei ic da a: , 75, WB189–WB202. d i:10.1190/1.3509468
- Sacchi, M., 1997, Re eigh i g a e gie i ei ic dec i i : I , 129, 651–656. d i:10.1111/j.1365-246X.1997. b04500.
- Sacchi, M. D., a d U i ch, T. J., 1996, E i a i f he di c e e F i a f , a i j e a i e i a ach: , 61, 1128–1136. d i:10.1190/1.1444033
- Sacchi, M., U i ch, T., a d Wa e , C., 1998, I e la i a de a la i n i g a high e l i d c e e F i e a f : , 46, 31–38. d i:10.1109/78.651165
- S i , S., 1991, Sei ic ace i a i i heF-Xd ai : , 56, 785–794. d i:10.1190/1.1443096
- T ad, D., 2009, Fi e di e i a i e lai : ec e i g f ac i i i c ai : , 74, V123–V132. d i:10.1190/1.3245216
- T ad, D., U i ch, T., a d Sacchi, M., 2002, Acc a e i e lai i h high e l i i e a Rad a f : , 67, 644–656. d i:10.1190/1.1468626
- a de Be g, E., a d F ied a de , M. P., 2009, P bi g he Pa e f i e f ba i i l i : I , 31, 890–912. d i:10.1137/080714488
- Wa g, Y., Ca , J., a d Ya g, C., 2011, Rec e f ei ic a efiq d ba ed c e i e e i g b a i i c ai ed egi e h da d he iece i e a d b a i i g: I , 187, 199–213. d i:10.1111/j.1365-246X.2011.05130.
- Wa g, Y., Li , P., Li , Z., S., T., Ya g, C., a d Zhe g, Q., 2013, Da a eg la i a i i g Ga ia bea dec i i a d a e : I , 21, 1–23. d i:10.1515/ji -2012-0030
- X , S., Zha g, Y., Pha , D., a d La ba e, G., 2005, A i ea age F i a a f f ei ic da a eg la i a i : , 70, V87–V95. d i:10.1190/1.1993713
- Ya g, Y., Ma , J., a d O he , S., 2012, Sei ic da a ec c i a i a i c i e i : UCLA CAM Re , 12–14.
- Z a je , P., a d Sacchi, M., 2007, F i e ec c i f if 1 a ied, a i ed ei ic da a: , 72, V21–V32. d i:10.1190/1.2399442